Fuzzy control for capacitor voltage balancing in a three-level boost converter using PV applications

[1*] Mohamadreza Samadi, [2]Seyed Mehdi RakhtAla

Abbreviations
MPPT: Maximum Power Point Tracking
FPI: Fuzzy Proportional Integral
TLBC: Three-Level Boost Converter
FLC: Fuzzy Logic Controller
PV: Photovoltaic
PFC: Power Factor Correction
PWM: Pulse Width Modulation
ESR: Equivalent Series Resistance
P&O: Perturb and Observe
INCond: Incremental Conductance Method
PI: Proportional Integral
V_{cont1}: Control voltage1
V_{cont2}: Control voltage2
V_{tri1}: Triangular voltage1
V_{tri2}: Triangular voltage2
V_L: Inductor voltage
V_{in}: Input voltage
V_O: Output voltage
T_S: Switching time

Abstract— **In this paper, MPPT control in PV systems is used by the FPI method which is an intelligent method. Further, the use of a TLBC as an interface converter instead of a conventional boost converter is examined in the PV system and a new transfer function of TLBC in terms of the mode of switching is verified. The main purpose of this paper is to balance voltage capacitors of TLBC by an intelligent fuzzy method. The rules of this controller are adjusted such that, in case of any disturbance in daylight and solar radiation, it can adjust the duty cycle TLBC, where voltage capacitors become well-adapted by being combined with MPPT controller. The simulation results verify the good performance of the proposed controller. Uncertainty parameters include the surrounding temperature, solar radiation, and output electric charge. The first two cannot be controlled by humans and may suddenly change by atmospheric conditions, while the third may suddenly change by the user and can be controlled by the proposed controller under any conditions. A dramatic change in the resistance electric charge is considered in this paper, where the voltage of capacitors does not have any overshoot or fluctuation. The simulation results verify that the capacitor voltage balance in the region is acceptable.**

***Index Terms*— Photovoltaic, Three-Level Boost Converter, FPI Controller, Intelligent Fuzzy Method.**

I. INTRODUCTION

Renewable energy sources such as PV power play a vital role in electric power generation and has become essential due to the shortage and environmental impacts of conventional fuels.
Hence, researchers have focused on new energies, in particular photovoltaics which has replaced fossil fuels.
The research performed on converters in photovoltaic systems can be summarized as follows. Park and co-workers in [1] presented a step-up DC/DC converter with a resonant double voltage. In Ref. [2], an interleaved multi-phase and multi-switch boost converter has been used for fuel cell applications. A novel high-efficiency DC/DC boost converter has been proposed in [3] to be used in photovoltaic systems. Other papers deal with the combinations of DC/DC converters, a high voltage step-up integrated double boost-sepic converter for fuel-cell and photovoltaic applications is presented in [4]. In Ref. [5] single-switch voltage equalizers using multi-stacked buck-boost converters have been proposed to settle the partial shading issues. The proposed voltage equalizers can be derived by stacking capacitor-inductor-diode filters on traditional buck-boost converters, such as SEPIC, Zeta, and Ćuk converters. The optimum equalization strategy has also been proposed and discussed for

[1*] Faculty of Electrical and Computer Engineering, Noshirvani University of Technology, Babol, Iran , * samadi_6947@yahoo.com
[2] Assistant Prof. in Faculty of Electrical Engineering, Golestan University, Gorgan, Iran, sm.rakhtala@gu.ac.ir

equalizers to compensate the partially shaded PV modules efficiently. In Ref. [6], the Buck-Boost has been used as a second converter after a Single-Ended Primary-Inductance Converter (SEPIC) which is controlled by a maximum power point tracking technique (MPPT). They have also indicated the importance of the output voltage regulation of photovoltaic systems. This method improves the efficiency of the photovoltaic system, ensures a good transfer of energy, and avoids the over-voltages risks which can negatively affect the load. In [7], the two-input buck converter has been proposed as the DC/DC stage for photovoltaic (PV) cascaded converters. This converter is attractive for this application because it is cost-effective and reliable and can achieve dual MPPT with only one power transistor. However, due to the simplified and integrated structure, the nonlinear characteristics of the converter and the two PV arrays complicate the control. Using a small-signal modeling, the control theme of the two PV voltages is formulated, and the effect of the nonlinearities is presented.

In this paper, a TLBC is used instead of a conventional boost converter. The TLBC demonstrated in Fig. 1 has drawn much attention to be used as an interface converter in PV systems. The TLBC has the advantages of low voltage stress, low inductor current ripple, and low switching loss [8-9]. Therefore, TLBCs are widely used in power electronic applications such as AC/DC PFC [8-9], DC/DC PV and control [10-12], fuel-cell [13-14], and wind energy [15].

For the conventional boost converter, the single switch needs to withstand the DC output voltage when the single switch is off. As demonstrated in Fig. 1, two cascaded switches and two cascaded capacitors are connected in series which are charged and discharged via switches. The blocking switch needs to withstand only half the DC output voltage if both capacitor voltages are balanced. If they are not balanced, however, one of the capacitor voltages may be larger than the breakdown voltage of the switch, which would damage the switch. Note that the inductor voltage in the TLBC has three levels, causing the TLBC to have a smaller inductor current ripple than the boost converter under the same switching frequency [16]. TLBCs are often utilized in high-voltage-ratio applications [11,14,17].

High-withstanding-voltage semiconductor switches often have higher costs and larger drain-source resistances than their low-withstanding-voltage counterparts. Thus, the TLBC enjoys the extra advantages of low switching loss and high efficiency [11].

The balance between two capacitor voltages should also be noted. In practice, mismatched capacitances and ESR would result in voltage imbalance.

The control of the TLBC should balance both capacitor voltages. The voltage-balancing control loop for TLBCs can be found in the literature [9-10], [12-13], [18-21]. The other voltage-balancing control can be found in the controls of the half-bridge PFC converter [22], [23] and the multilevel inverter [24],[25]. Fig. 1 illustrates a schematic representation of the proposed system employing TLBC.

A proportional controller is usually utilized for balancing the voltage capacitors of TLBC in a PV system [26]. Use of the PI controller alone cannot accurately trace capacitor voltage balance because of parametric uncertainty, disturbances, and noises. Algorithms which can achieve an appropriate gain are usually connected to the PI controller in series. This requires two controllers, increasing the complexity of the circuit and failing to appropriately respond to uncertainty parameters. However, the use of the proposed fuzzy controller is easier and more appropriate for non-linear systems, contributing to achieving a more accurate tracing for uncertainty parameters without requiring other complex algorithms.

In this paper, an MPPT controller was proposed with an intelligent FPI method. The main purpose of the present study was to balance voltage capacitors with minimal errors in different cases of sudden changes in the temperature of the sun, solar radiation, and electric charge, using FLC. This controller is very simple, robust, and suitable for nonlinear systems. Nevertheless, FPI is a knowledge-based controller which does not require any theoretical approach to design a control law and can balance capacitor voltages well under different climatic conditions. Given the PV structure which is influenced by environmental conditions, temperature fluctuations and solar radiation, as common uncertainty parameters, affect this system. To overcome these uncertainties, the use of a fuzzy logic intelligent controller can be a good choice due to its internal structure. This controller fulfills this by changing the duty cycle. It has a very minor error, which is below 0.2 V, and the capacitor voltage balance is acceptable in the region.

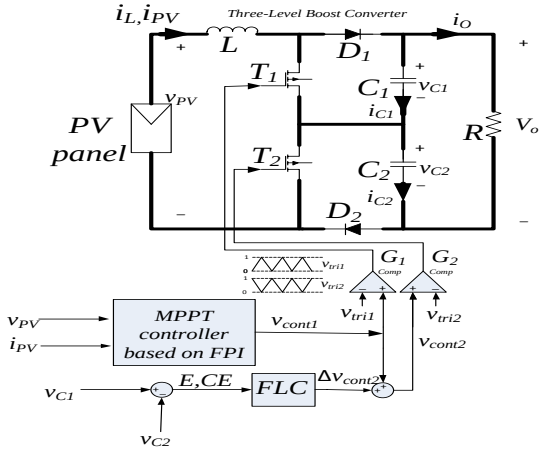

Fig. 1. Three-level boost-type converter with the MPPT control and voltage balancing control connected to PV

II. PV PANEL MODELING

The equivalent circuitry of a PV cell is shown in Fig. 2 , in which the simplest model can be represented by a current source antiparallel to a diode [27]. The non-idealities are represented by the insertion of resistances *Rs* (series resistance) and *Rp* (Parallel resistance).

The PV panel simulation model is based on the output current of one PV equivalent model, and its mathematical equation is represented by:

$$I = I_{ph} - I_r \cdot \left[e^{q.\frac{V+I.R_S}{\eta.k.T}} - 1 \right] - \frac{V + I.R_S}{R_P} \quad (1)$$

where V represents the output PV voltage of one PV panel, I_{ph} is the photocurrent, I_r is the saturation current, q denotes the electrical charge (1.6×10^{-19} C), η indicates the P-N junction quality factor, k is the Boltzmann constant (1.38×10^{-23} J/K), and T is the temperature (in Kelvin). The PV electrical parameters are presented in Table I.

TABLE I
ELECTRICAL PARAMETERS OF THE PV MODULE

Maximum Power	$\mathbf{P_{MAX}}$=*83.05W*
Voltage at MPP	$\mathbf{V_{MPP}}$=*17.15V*
Current at MPP	$\mathbf{I_{MPP}}$=*4.85A*
Open Circuit Voltage	$\mathbf{V_{OC}}$=*21.2V*
Short Circuit Current	$\mathbf{I_{SC}}$=*5.27A*
Temperature Coefficient of $\mathbf{I_{sc}}$	**α**=*0.65*10^{-3}A/°C*

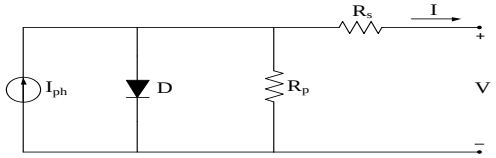

Figure 2: Equivalent model of the PV cell

III. THREE-LEVEL BOOST-TYPE CONVERTER

As depicted in Fig. 1, the switching signal G_1 is obtained from the comparison of the control signal v_{cont1} with the triangular signal v_{tri1}. Due to the low output voltage ripple, V_O is assumed constant. V_O is the TLBC output voltage which is assumed constant due to using a constant resistance. Therefore, the sum of two capacitor voltages will be fixed $v_{C1} + v_{C2} = V_O$.

In addition, the other switching signal G_2 is obtained by comparing the control signal v_{cont2} with the triangular signal v_{tri2} where there is a phase difference of 180° between the two triangular signals.

Because of the presence of the input inductor L and two diodes D_1 and D_2 in the TLBC, both switches can be turned on at the same time. There are four possible Switching States, as shown in Fig. 3.

Based on Fig. 3(a), both switches turn on when the control signal v_{cont1} is larger than the signal $v_{cont1} \geq v_{tri1}$ and the control signal v_{cont2} is larger than the signal $v_{cont2} \geq v_{tri2}$.

Thus, the inductor voltage v_L is equal to the PV voltage $v_L = V_{PV} \geq 0$. The current rising rate in Switching State 1 is always positive. For Switching State 2, as shown in Fig. 3(b), the upper switch T_1 turns on and the lower switch T_2 turns off. The inductor voltage v_L is equal to the difference between the PV voltage v_{PV} and the capacitor voltage $v_L = v_{PV} - v_{C2}$. The current rising rate may be either positive or negative. Additionally, the capacitor current i_{C2} is equal to the inductor current $i_{C2} = i_L \geq 0$. Thus, capacitor C_2 is charging and the other capacitor C_1
is discharging in Switching State 2.

Similarly, as shown in Fig. 3(c), when the upper switch T_1 turns off and the lower switch T_2 turns on, the inductor voltage v_L is equal to the voltage difference $v_L = v_{PV} - v_{C1}$ and the current rising rate may be either positive or negative. It is also noted that, in Switching State 3, capacitor C_1 is charging and the other capacitor C_2 is discharging.

According to Fig. 3(d), when both switches turn off, the inductor voltage v_L is equal to the PV voltage minus the output voltage $v_L = v_{PV} - V_O = v_{PV} - v_{C1} - v_{C2}$. Since the output voltage is higher than the input voltage in the boost-type converter, the current rising rate is always negative in switching state 4.

All the capacitor currents in various switching states are tabulated in Table II.

In Fig. 1 is shown, PV is connected to Three-level boost-type converter with the MPPT control and voltage balancing control. The aim of this controller based on MPPT is, maximum power tracking of PV. In Fig. 1 is depicted that V_{C1} and V_{C2} are compared of a comparator and voltage difference is obtained.

The voltage difference entered to FLC controller and the FLC output is added to v_{cont1} and generates v_{cont2}.

The obtained signal is compared with signal v_{tri2} (there is a 180° phase difference between v_{tri2} and v_{tri1}). The obtained signal G_2 enters into the second switch. In this way, two rates of v_{cont1} and v_{cont2} will be created which have half the period of the phase difference.

v_{cont2} denotes the control voltage resulting from the combination of MPPT and TLBC capacitor voltage balances. It creates the duty cycle, ranging from 0 to 1, which is required for the second switch. By doing so, the three-level voltage is obtained in the output converter which not only increases the input voltage, but also decreases the switch voltage stress. It can also decrease the filter size by increasing frequency. In this paper, the balance of the capacitor voltage of TLBC is explained. Its single disadvantage is imbalanced voltage capacitors which can be corrected and balanced by FLC.

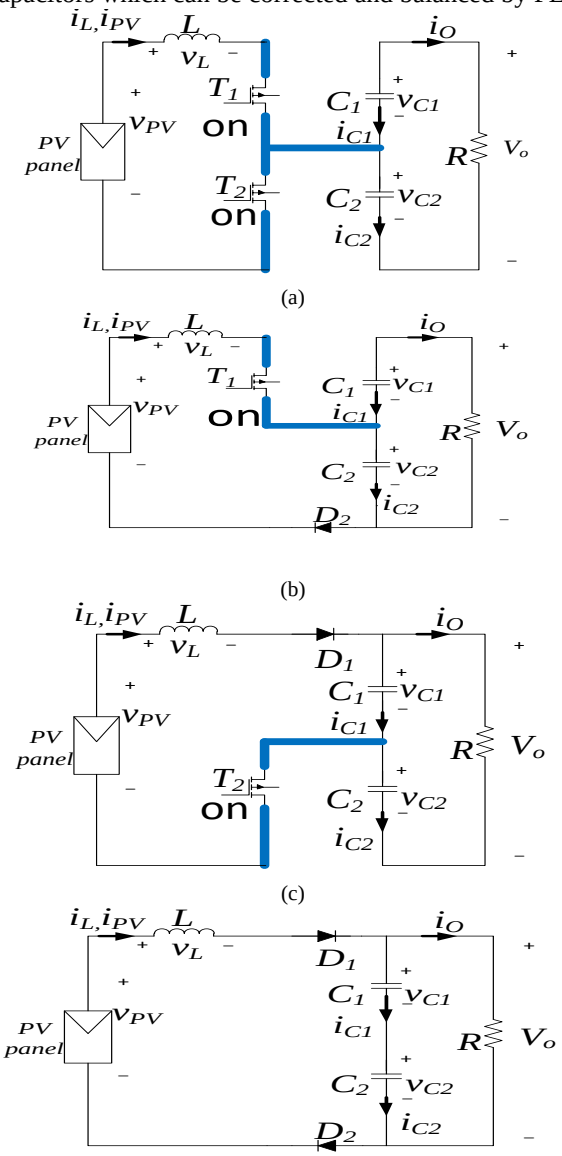

Fig. 3. Possible switching states in three-level boost-type converter: (a) state 1; (b) state 2; (c) state 3 and (d) state 4

TABLE II
CAPACITOR CURRENTS IN EACH STATE

		State 1	State 2	State 3	State 4
$1<v_{cont1}+v_{cont2}<2$	i_{C1}	$-i_O < (0)$	$-i_O < (0)$	$i_L-i_O > (0)$	
	i_{C2}	$-i_O < (0)$	$i_L-i_O > (0)$	$-i_O < (0)$	
$0<v_{cont1}+v_{cont2}<1$	i_{C1}		$-i_O < (0)$	$i_L-i_O > (0)$	$i_L-i_O > (0)$
	i_{C2}		$i_L-i_O > (0)$	$-i_O < (0)$	$i_L-i_O > (0)$

IV. NEW THREE-LEVEL BOOST CONVERTER VOLTAGE CONVERSION RATES

Obtaining the voltage conversion rate of TLBC, similar to obtaining the voltage conversion rate of the conventional boost converter [28], is done using the average inductor voltage of the switching period.

The average inductor voltage is zero at the steady state. However, to study the TLBC, because the two switches are simultaneously turned on or off for three voltage levels, there are two conditions: condition $0 < v_{cont1} + v_{cont2} < 1$ and the condition $1 < v_{cont1} + v_{cont2} < 2$.

Condition $1 < v_{cont1} + v_{cont2} < 2$:

In condition $1 < v_{cont1} + v_{cont2} < 2$, as already mentioned; only modes 1, 2, and 3 occur, as shown in Fig. 4(a). Control signals are between 0 and 1 ($0 < v_{cont1} < 1$ and $0 < v_{cont2} < 1$) according to PWM signal. In this conditions, $v_{cont1} + v_{cont2} > 1$ and $v_{cont1} \neq 0$ and $v_{cont2} \neq 0$ and it means that T_1 and T_2 are not OFF. Modes 1, 2, and 3 occur, and there is not mode 4 as shown in Fig. 4(d).

In Fig. 4(a), switching signals of T_1 and T_2 have equal width with a phase difference of 180°.

Fig. 4(a) illustrates the switching TLBC. By equating the $\boldsymbol{v_{cont1} = v_{cont2} = D}$ and $D > 0.5$, the above condition is met. Now, turn to the proof of the relationship:

$$D_1 = \frac{2D-1}{2} \tag{2}$$

$$\bar{V_L} = 0 \rightarrow$$

$$\frac{2}{T_S}((V_{in} - \frac{V_o}{2}).(1-D) + V_{in}.D_1).T_S = 0$$

$$2(V_{in}.D - \frac{V_{in}}{2} + V_{in} - \frac{V_o}{2} - V_{in}.D + \frac{V_o}{2}.D) = 0$$

$$V_{in} = V_o.(1-D) \Rightarrow \frac{V_o}{V_{in}} = \frac{1}{1-D} \tag{3}$$

In condition $0 < v_{cont1} + v_{cont2} < 1$, as mentioned before, only modes 2, 3, and 4 occur, as depicted in Fig. 4(b) and never will not happen $v_{cont1} + v_{cont2} > 1$ and v_{cont1} and v_{cont2} will not equal 1.

Fig. 4(b) demonstrates the switching TLBC. By equating the $\boldsymbol{v_{cont1} = v_{cont2} = D}$ and $D < 0.5$, the above condition is met. Following equation shows the proof of the relationship:

$$D_1 = \frac{1-2D}{2} \tag{4}$$

$$\bar{V_L} = 0 \rightarrow$$

$$\frac{2}{T_S}((V_{in} - \frac{V_o}{2}).D + (V_{in} - V_o).D_1).T_S = 0$$

$$2(\frac{V_{in}}{2} - \frac{V_o}{2} + \frac{V_o}{2}.D) = 0$$

$$V_{in} = V_o.(1-D) \Rightarrow \frac{V_o}{V_{in}} = \frac{1}{1-D}$$

Therefore, Eq. 3 is achieved.

If v_{cont1} and v_{cont2} are equal, the duty cycle is constant. It is obvious that the three-level boost-type converter with constant duty cycles has a voltage conversion rate similar to that of conventional boost-type converters (which is true based on Eq. 3).

In fact, the TLBC transfer function is exactly equivalent to that of the conventional boost converter. However, the overall deductive voltage conversion rate for $\boldsymbol{v_{cont1} \neq v_{cont2}}$ is reviewed.

In the case of $1 < v_{cont1} + v_{cont2} < 2$ in Fig. 4(c), the conducting times of Switching State 2 and Switching State 3 are $(1 - v_{cont2})T_s$ and $(1 - v_{cont1})T_s$, respectively. The remaining time for Switching State 1 is $(v_{cont1} + v_{cont2} - 1)T_s$. Every Switching States are shown clearly in Fig. 4(d). The inductor average voltage in this case is calculated in following:

$$\bar{V_L} = 0 \rightarrow$$

$$\frac{1}{T_S}((1-v_{cont1}).T_S.(V_{in} - \frac{V_o}{2}) + (v_{cont1} + v_{cont2} - 1).T_S.V_{in}$$

$$+ (1-v_{cont2}).T_S.(V_{in} - \frac{V_o}{2}) = 0$$

$$\frac{V_o}{V_{in}} = \frac{1}{1 - \frac{1}{2}v_{cont1} - \frac{1}{2}v_{cont2}} \tag{5}$$

Similarly, for the other case of 0 <v_{cont1} + v_{cont2} <1 in Fig. 4(d), the conducting times of Switching States 2 and 3 are $v_{cont1}T_s$ and $v_{cont2}T_s$, respectively. The remaining time for Switching State 4 is $(1 - v_{cont1} - v_{cont2})Ts$. The average of inductor voltage in TLBC is calculated in following:

$$\bar{V_L} = 0 \rightarrow$$

$$\frac{1}{T_S}((1-v_{cont1}-v_{cont2}).T_S.(V_{in}-\frac{V_o}{2})+v_{cont1}.T_S.(V_{in}-\frac{V_o}{2})$$

$$+v_{cont2}.T_S.(V_{in}-\frac{V_o}{2})=0 \Rightarrow$$

$$\frac{V_o}{V_{in}}=\frac{1}{1-\frac{1}{2}v_{cont1}-\frac{1}{2}v_{cont2}}$$

We will precisely achieve Eq. 5.

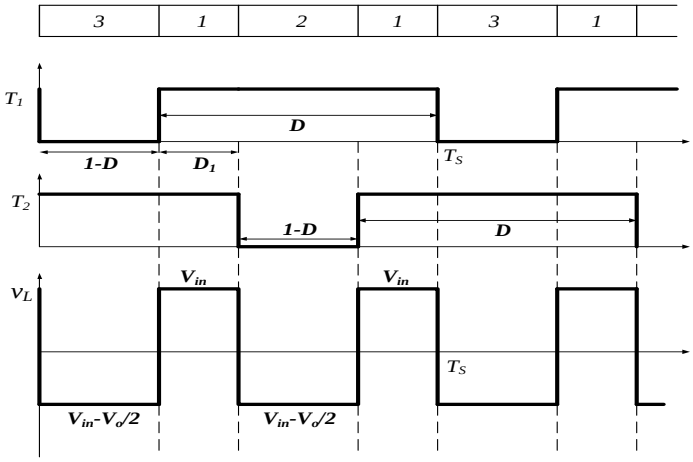

Fig. 4(a). Inductor voltage waveform and the switching of modes 1 <v_{cont1} + v_{cont2} <2

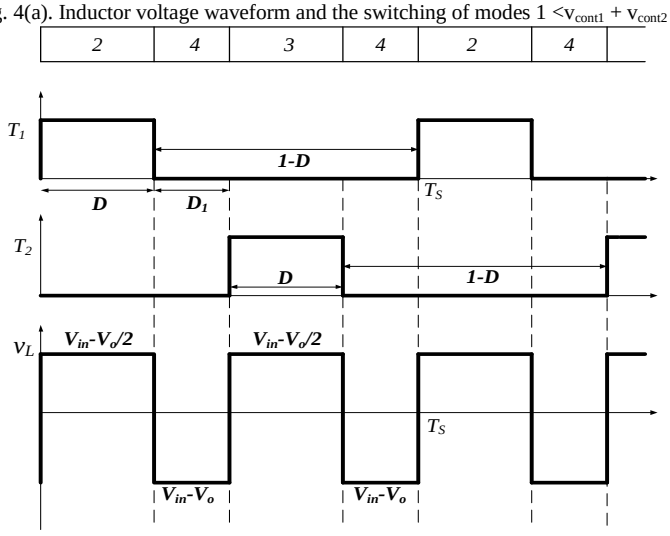

Fig. 2(b). Inductor voltage waveform and the switching of modes 0 <v_{cont1} + v_{cont2} <1

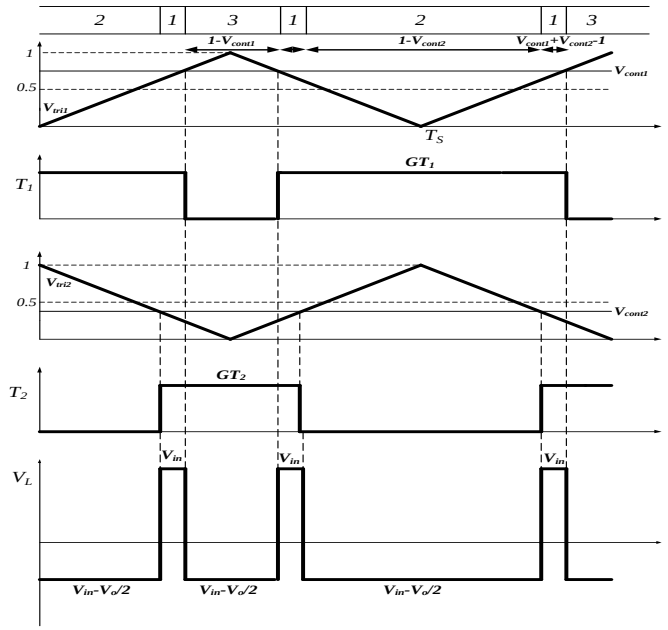

Fig. 4(c). Behavior of the three-level boosting converter in $1 < v_{cont1} + v_{cont2} < 2$

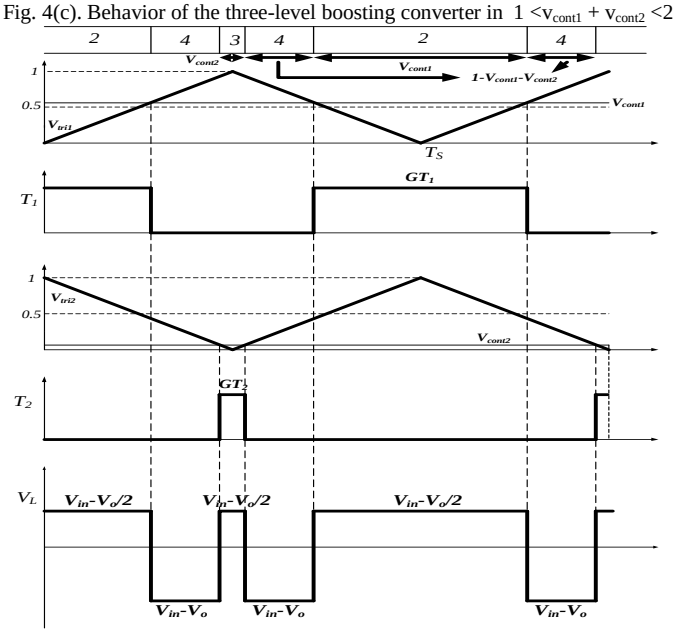

Fig. 4(d). Behavior of the three-level boosting converter in $0 < v_{cont1} + v_{cont2} < 1$

V. MPPT ALGORITHMS

Numerous MPPT algorithms have been developed and implemented by researchers [29,30]. In general, the MPPT techniques can be divided into two categories: direct and indirect methods [31]. The direct method of MPPT algorithms is independent of prior knowledge of PV modules' characteristics. MPPT algorithms included in this category are P&O, INCond, feedback voltage or current, and FLC method. The indirect method, on the other hand, requires prior evaluation of the PV generator. It is based on the mathematical relations obtained from empirical data. Methods such as look-up table, open-circuit PV voltage, short-circuit PV current, and other MPPT algorithms are examples of the indirect method [31-33].

A. MPPT with FPI controller

The reasons for using the FPI controller as compared with conventional controllers are mentioned as follows:

1) Utilizing two controllers instead of one controller increases the precision in a closed loop system. Due to its simplicity, fuzzy controller is easier, compared with other complicated algorithms.

2) Compared to classic controllers, it is more intelligent, robust, and suitable for systems with model uncertainty, parametric uncertainty, and disturbances.

3) Fuzzy controller is applicable to multi input- multi output (MIMO) systems, but conventional controllers like PID are not applicable to MIMO systems and are used only for single input-single output (SISO) systems.
The FLC provides high performance even if the load as a disturbance and parameters of the model change [34]. The main advantage of FLC methods compared with other classical control techniques is their lower dependency of the accurate mathematical model and nominal parameters. In this regard, it was reportedly [35] more suitable for the MPPT process, especially for rapidly changing atmospheric conditions.
However, FPI controller have also some disadvantages as follows:
1) needing trial and error to define the membership functions;
2) High implementation costs;
3) Complex calculation of the controller;
4) Use of two controllers enhances the precision, but the model makes the system more complex.
In this paper, for the MPPT with FPI, we have used Fig. 5 for simulation. As can be seen from the figure and similar to the MPPT with fuzzy methods, FLC inputs are error E(k) and error changes CE(k) with their equations presented in (6) and (7). FLC outputs are the values of K_P and K_I which, after adjustment, enter the PI controller. They exhibit maximum power, which is oscillation-free and completely smooth, even better than the conventional fuzzy method.
The function of this FLC with PI adjustment can be classified into four elements: fuzzification, rule base, inference engine, and defuzzification.

$$E(k)=\frac{P_{pv}(k)-P_{pv}(k-1)}{V_{pv}(k)-V_{pv}(k-1)} \tag{6}$$

$$CE(k)=E(k)-E(k-1) \tag{7}$$

A.1. Fuzzification
Membership function values are assigned to linguistic variables using seven fuzzy subsets: NB (negative big), NM (negative medium), NS (negative small), ZO (zero), PS (positive small), PM (positive medium), and PB (positive big). The partition of fuzzy subsets and the shape of membership functions, which can appropriately adjust the system, are demonstrated in Fig. 6.

A.2. Fuzzy Inference System
The inference engine mainly consists of a fuzzy rule base and fuzzy implication sub-blocks. The inputs which are now fuzzified are fed to the inference engine and the rule base is then applied. The output fuzzy set is identified using the fuzzy implication method. Here, we use the MIN-MAX fuzzy implication method [36]. Tables III and IV show the rule base of the FLC to adjust the amount of K_P and K_I.

A.3. Defuzzification
For this system, the center-of-gravity method is selected to compute the output of this FLC which is the same as PI value changes.
By the changes of the value of PI in the output of FLC, the control signal is generated using PWM and enters the MOSFET switch in TLBC.
Duty cycle changes occur according to Equation (8). Since $\Delta v_{cont1}(k) = v_{cont1}(k) - v_{cont1}(k-1)$ is. With the accumulation of signal $\Delta v_{cont1}(k)$ with $v_{cont1}(k-1)$ of simulation, signal $v_{cont1}(k)$ is given to the TLBC switch control.

$$\Delta v_{cont1}=\frac{\sum_{j=1}^{n}\mu(v_{cont1\,j}).(v_{cont1\,j})}{\sum_{j=1}^{n}(v_{cont1\,j})} \tag{8}$$

Table III
Fuzzy rule table for K_P

CE / E	NB	NM	NS	ZO	PS	PM	PB
NB	*PB*	*PB*	*PB*	*PM*	*PS*	*ZO*	*ZO*
NM	*PB*	*PB*	*PM*	*PS*	*PS*	*ZO*	*NS*
NS	*PM*	*PM*	*PM*	*PS*	*ZO*	*NS*	*NS*
ZO	*PM*	*PM*	*PS*	*ZO*	*NS*	*NM*	*NM*
PS	*PS*	*PS*	*ZO*	*NS*	*NS*	*NM*	*NM*
PM	*PS*	*ZO*	*NS*	*NM*	*NM*	*NM*	*NB*
PB	*ZO*	*ZO*	*NM*	*NM*	*NM*	*NB*	*NB*

Table IV
Fuzzy rule table for K_I

CE / E	NB	NM	NS	ZO	PS	PM	PB
NB	*NB*	*NB*	*NM*	*NM*	*NS*	*ZO*	*ZO*
NM	*NB*	*NB*	*NM*	*NS*	*NS*	*ZO*	*ZO*
NS	*NB*	*NM*	*NS*	*NS*	*ZO*	*PS*	*PS*
ZO	*NM*	*NM*	*NS*	*ZO*	*PS*	*PM*	*PM*
PS	*ZO*	*ZO*	*ZO*	*NS*	*NS*	*ZO*	*ZO*
PM	*NS*	*NS*	*NS*	*NS*	*ZO*	*ZO*	*ZO*
PB	*ZO*	*ZO*	*ZO*	*ZO*	*ZO*	*ZO*	*ZO*

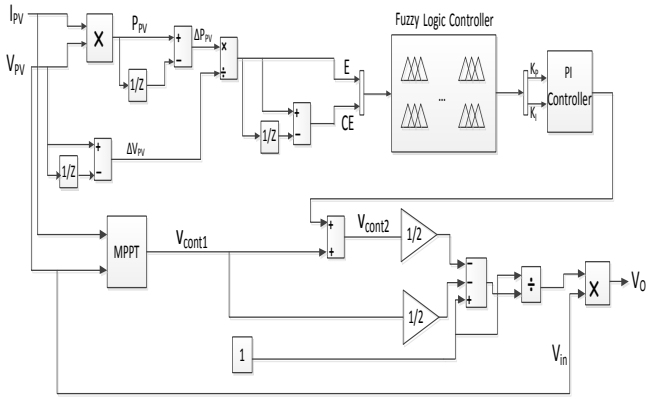

Fig. 5. Simulation controllers FPI

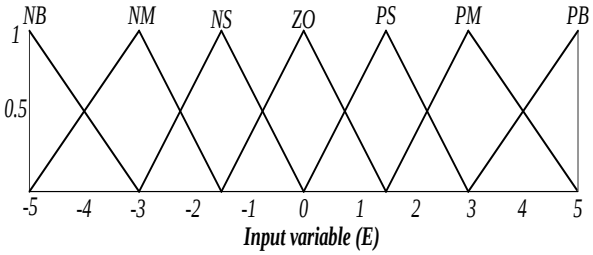

(a)

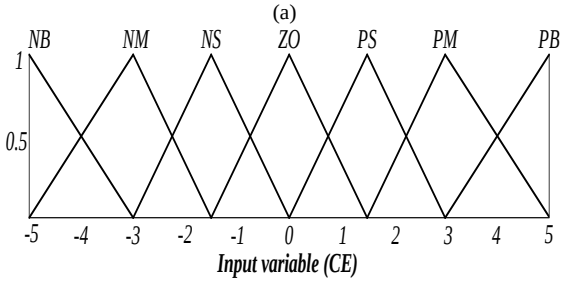

(b)

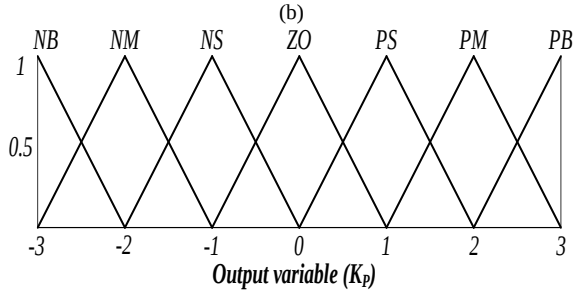

(c)

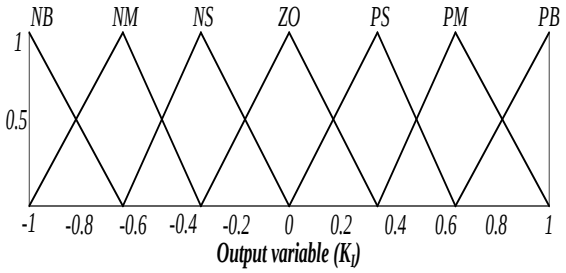

(d)

Fig. 6. Membership function plots for (E), (CE), (K_P), (K_I)

VI. PROPOSED VOLTAGE BALANCING CONTROL

The voltage-balancing control loop is plotted in Fig. 7, where the difference between the two values is the input to a fuzzy logic controller to obtain the signal Δv_{cont2} . Then, the control signal v_{cont2} is obtained by:

$$V_{cont2} = V_{cont1} + \Delta V_{cont2} \tag{9}$$

A. Fuzzy logic controller

The FLC inputs in this part of the controlled systems are the error voltage of capacitors E (K) and error changes CE (K). The output of FLC includes Δv_{cont2} changes whose fuzzy rules act such that the voltage differences become zero with Δv_{cont2} changes. The fuzzy logic controller, which is proposed in this paper, is the same as the MPPT controller for adjusting K_P quotient, represented as Figs. 6(a)-6(c) with rule bases of Table III of the previous section. This controller well adjusts Δv_{cont2} and is added to the v_{cont1} signal obtained from the MPPT controller. This controlling method appropriately balances voltage capacitors under different conditions of radiation and ambient temperature. Fig. 8 demonstrates the proposed flowchart diagram of FLC.

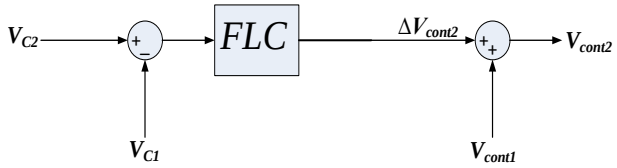

Fig. 7. voltage balancing control loop

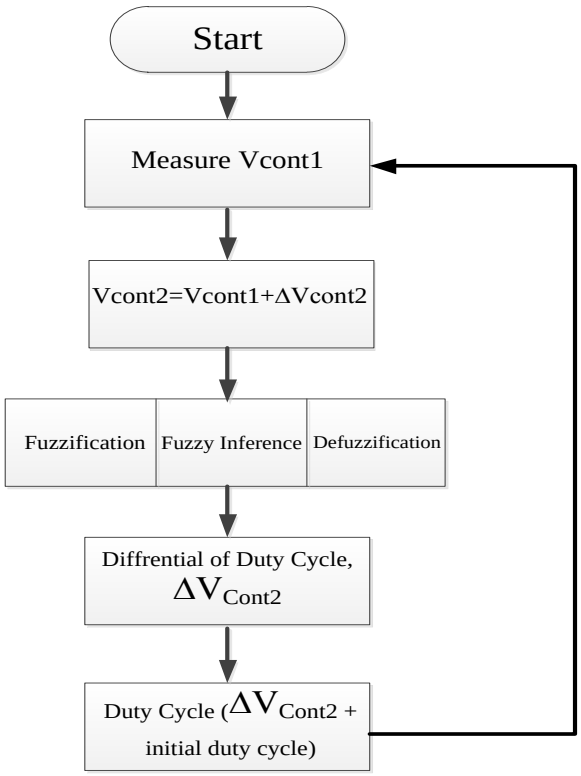

Fig. 8. Proposed flowchart diagram of FLC

VII. RESULTS AND DISCUSSION

The simulated parameters are listed in Table V. Two capacitors $C_1 = C_2 = 2000\ \mu$F were connected in series in the circuit to induce voltage imbalance. The frequency of the voltage-balancing loop was 10 KHz. The output voltage of TLBC is displayed in Fig. 9. The newly-designed TLBC increased the converter output voltage of the PV panels from 17.15 V to 126 V. According to Equation (3), which was verified for TLBC, the output voltage was almost seven times larger than the input voltage. The proposed controller maintained v_{cont1} and v_{cont2} constant at about 6/7. This pulse width enhanced the output voltage by up to 7 times the input voltage.

Although this increase was significant, it did not damage TLBC switches. In what follows, the results of the design of the proposed controller for balancing the voltage of TLBC capacitors will show that this value for voltage was exactly divided at the beginning of the simulation and would branch into two TLBC switches, thereby decreasing switch life and seriously damaging the switches.

If the input voltage of the conventional boost-type controller is increased by seven times, we will require a switch which can resist a 7-fold input voltage, i.e. a switch with a higher nominal voltage, which reduces the switch life and raises the switch costs due to the high voltage rate. Nevertheless, using TLBC, we can increase the input voltage by seven times. Then, with the help of the proposed controller which is designed for balancing of voltage of capacitors, we can impose this voltage rise on two switches with low voltage rates (lower nominal voltages) and lower costs which can resist half this voltage growth (i.e. 3.5 times) [14].

Thus, TLBC is far better for a high voltage rate and high power, where switches with a lower voltage capacity can be employed.

Fig. 10 illustrates the characteristics of the power of the photovoltaic panels with MPPT controller FPI. It can be observed that this controller appropriately tracked the reference power, while its maximum error was 0.02 W. This type of tracking results in a power transfer to the output with very little loss, while the value of the duty cycle is kept constant.

In order to check the accuracy of the proposed controller in balancing the voltage of TLBC capacitors in a PV system, it was evaluated with a desired value and set point.

Fig. 11(a) presents the simulation of the voltage balancing of reference TLBC capacitors by the fuzzy controller method.

In Fig. 11(a), V_{dc1} and V_{dc2} represent the voltage of capacitors in TLBC connected to a three-level inverter with different initial voltages.

As the figure shows, the voltage of the two capacitors has a high voltage overshoot for reaching a certain voltage in the beginning of simulation until reaching that point, which can interrupt power switches. It is not clear how much overshoot it produces for higher voltages. This growth of error hinders the system and increases the risk.

Fig. 11(b) displays the TLBC voltage capacitor based on PI controller of Ref. [38]. It is clear that the existence of any disturbance in the system causes V_{C1} and V_{C2} imbalance, and there are differences between V_{C1} and V_{C2}. Furthermore, there is no undershoot and overshoot in the transient time with PI controller.

Fig. 11(c) exhibits the TLBC voltage capacitor based on self-tuning fuzzy PI controller of Ref. [39]. It is clear that there are great fluctuations on the Vc_1 and Vc_2. These fluctuations act as impulses with high amplitude which is a major issue for this controller. As reveal in Fig. 12(a) to Fig. 12(d), the capacitor voltage balancing based on the proposed FLC controller has been regulated suitably and more robust than PI and self-tuning fuzzy PI controller.

Fig. 12(a) depicts the simulation of voltage balancing of TLBC controllers with the proposed controller. As can be seen, from the start of simulation, the two voltage capacitors tracked each other and were equal in terms of voltage value. Tracking was highly precise and accurate, and errors observed in the magnified section did not exceed 0.2 V.

To check the accuracy of the proposed controller, we simulated it under abrupt solar radiation. Based on Fig. 12(b), when solar radiation varied abruptly from 1000 W/m^2 to 500 W/m^2 (as uncertainties which are possible in environmental settings), the proposed controller worked well and no problems were detected in setting up and tracking. Fig. 12(c) reveals the case when both solar radiation and temperature changed abruptly as two uncertainties. In the simulation test, although solar radiation suddenly changed from 1000 W/m^2 to 700 W/m^2 in 0.4 seconds and temperature from 45 °C to 15 °C in 0.7 seconds, the voltage of capacitors was highly intelligent and no problems occurred.

Fig. 12(d) illustrates the voltage balancing of TLBC capacitors at the sudden change in resistance electric charge as another uncertain parameter. Based on this figure, at the sudden change of resistance charge from 200 Ω to 50 Ω within 0.3 seconds, the voltage of capacitors did not have any overshoot or fluctuation, reacted immediately, and had an accurate tracking. Accordingly, the proposed controller ensures that no overshoot occurs in the worst uncertainties and tracking is absolutely perfect.

Table V
PARAMETERS OF PV-FED THREE-LEVEL CONVERTER

Output Voltage	*126V*
Inductor L	*0.75mH*
Capacitor C_1=C_2	*2000μF*
Switching period T_s	*100μs*
Controller parameter K_p	*0.155*

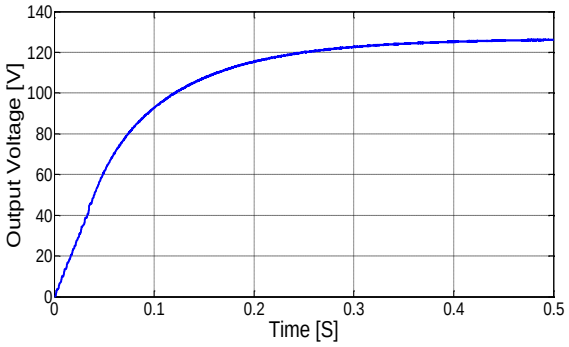

Fig. 9. Output Voltage of TLBC

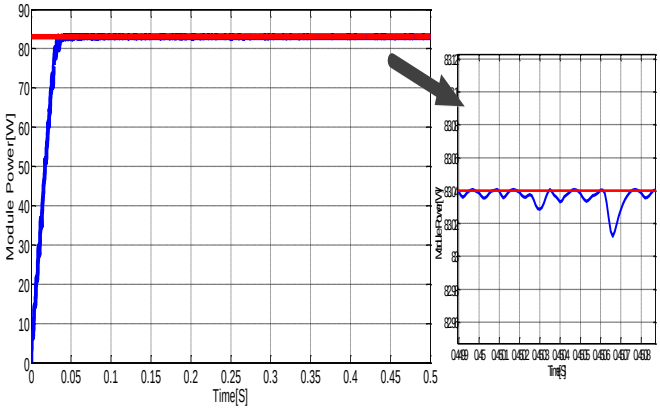

Fig. 10. PV power curves generated by FPI controller

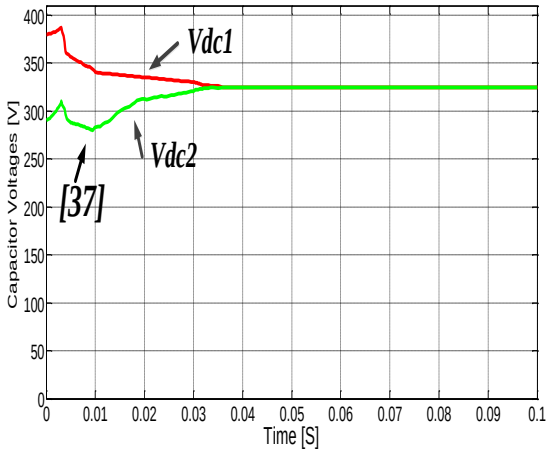

Fig. 11(a). Capacitor voltages with FLC [37]

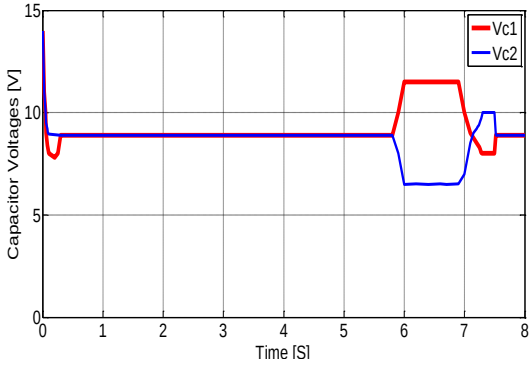

Fig. 11(b). Capacitor voltages with PI[38]

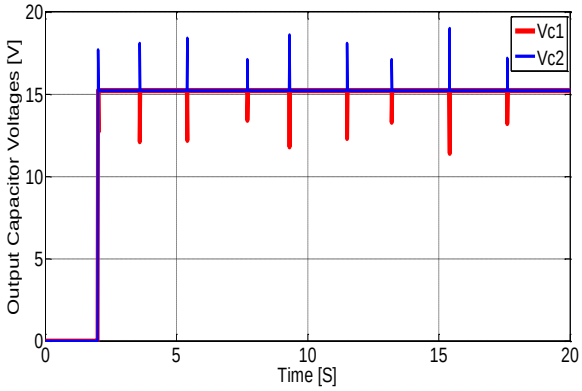

Fig. 11(c). Capacitor voltages with self-tuning fuzzy PI [39]

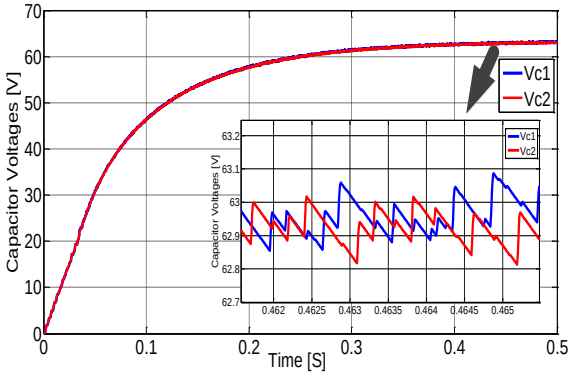

Fig. 12(a). Capacitor voltages by FLC in 25°c,1000W/m^2

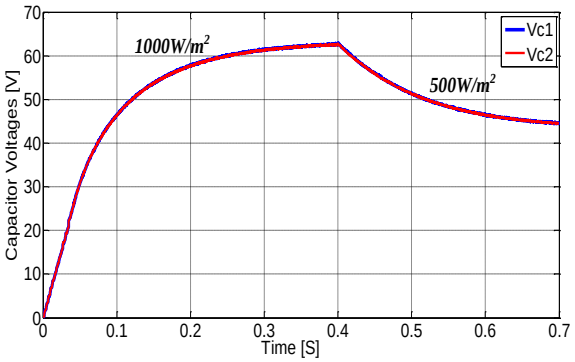

Fig. 12(b) Capacitor voltages in the presence of radiation sudden change, as uncertainty by FLC.

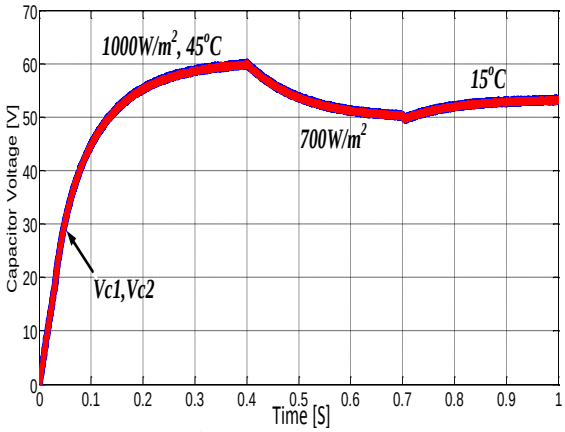

Fig. 12(c). Capacitor voltages in the presence of radiation and temperature sudden change, as uncertainty by FLC.

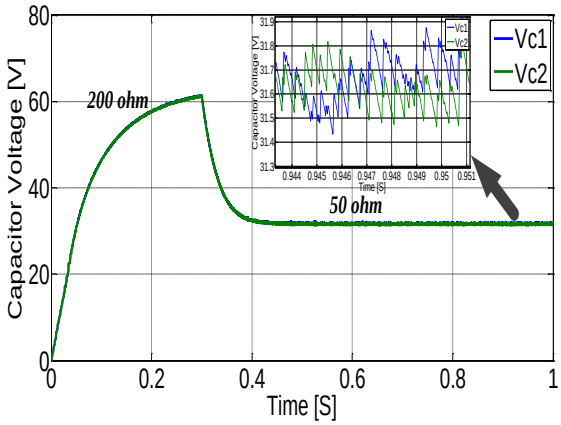

Fig. 12(d). Capacitor voltages in the sudden change resistive load as uncertainty by FLC.

VIII. CONCLUSIONS

In this paper, a new transfer function of TLBC was verified in terms of the mode of switching. MPPT control was performed by an intelligent FPI. The main objective was to balance the voltage of capacitors of the TLBC in the PV system in which FLC was utilized. This controller written by appropriate changes in duty cycle rate by rules and by being combined with signals obtained from MPPT acted in a way that, in case of sudden changes in daylight, solar radiation, and output resistance charge, the balancing of voltage capacitors of TLBC would occur appropriately and the error would be below 0.2 V. The proposed FLC controller was compared to PI and self-tuning fuzzy PI for capacitor voltage balancing of TLBC. It was observed that the PI controller has a voltage difference of about 5 V within between 6 and 7 s. Also, there was an overshoot of about 1 V in the start of simulation. For self-tuning fuzzy PI, there is some variation in results which is a major issue.

In this paper, balance voltage capacitors of TLBC were considered in four scenarios by an intelligent fuzzy method under uncertainty parameters such as the surrounding temperature, solar radiation, and output electric charge. The scenarios include:

A. Comparison between different controllers:

In the first scenario, the proposed controller was compared to PI and self-tuning fuzzy PI for capacitor voltage balancing of TLBC. It was found that the last studies have some problem such as overshoot and undershoot of about 1 V and there is some variation in results which is a major issue.
However, balancing of the voltage capacitors with minimal errors in different cases was done by the proposed intelligent controller.

B. Sudden changes in the solar radiation:

The atmospheric conditions suddenly change as disturbances. This problem can be controlled by the proposed controller under any conditions. The capacitor voltage balancing is managed with minimal errors in this case of dramatic changes and there is not any overshoot and undershoot between the capacitor voltages of TLBC.

C. Changes in the temperature and solar radiation:

The temperature and solar radiation fluctuations are common uncertainty parameters. To resolve these uncertainties, the intelligent controller overcame these problems.

D. Changes in the load disturbance:

The sudden change in the resistance electric charge was considered as the load disturbance, where the capacitor voltage did not have any overshoot fluctuation. The results in figures verify the acceptable range of capacitor voltage balance.
The simulation results clearly suggested better performance of the proposed controller. The controller can also be used for systems with an unstable voltage. So, further studies are warranted to confirm the applicability of the results to practical implementation in a closed loop system.

REFERENCES

[1] Park Jae-Kyu, Choi Woo-Young, Kwon Bong-Hwan,"Step-up DC-DC converter with a resonant voltage doubler" IEEE Transaction Industrial Electronic, vol. 54(6), PP.3267-3275, 2007.
[2] Garrigos Ausias, Sobrino-Manzanares Fernando, "Interleaved multi-phase and multi-switch boost converter for fuel cell applications" International Journal of Hydrogen Energy, vol.40, PP.8419-8432, 2015.
[3] Fathabadi Hassan, "Novel high efficiency DC/DC boost converter for using in photovoltaic systems" Solar Energy, vol.125, PP. 22-31, February 2016.
[4] Sabzali Ahmad J, Ismail Esam H, Behbehani Hussain M, "High voltage step-up integrated double Boost-Sepic DC-DC converter for fuel-cell and photovoltaic applications" Renewable Energy, vol.82, PP.44-53, October 2015.
[5] Masatoshi Uno, Akio Kukita, "Single-Switch Voltage Equalizer Using Multi-Stacked Buck-Boost Converters for Partially-Shaded Photovoltaic Modules "IEEE Transaction on Power Electronis, vol.30, PP. 3091 – 3105, June 2015.
[6] Mohamed Kaouane, Akkila Boukhelifa, Ahmed Cheriti, "Regulated output voltage double switch Buck-Boost converter for photovoltaic energy application" International Journal of Hydrogen Energy, vol.41, PP.20847-20857, Dec 2016.
[7] Andoni Urtasun, Dylan Dah-Chuan Lu, "Control of a Single-Switch Two-Input Buck Converter for MPPT of Two PV Strings " IEEE Transaction Industrial Electronic, vol.62, PP. 7051–7060, May 2015.
[8] Hung-Chi Chen, Jhen-Yu Liao, "Modified Interleaved Current Sensorless Control for Three-Level Boost PFC Converter with Considering Voltage Imbalance and Zero-Crossing Current Distortion", IEEE Transaction Industrial Electronic, vol. 62, PP. 6896 – 6904, 2015.
[9] Mutharath Rajesh, Bhim Singh, "Analysis, design and control of single-phase three-level power factor correction rectifier fed switched reluctance motor drive", IET Power Electronics., vol. 7, PP. 1499 – 1508, June 2014.
[10] J. M. Kwon, B. H. Kwon, and K. H. Nam, "Three-Phase photovoltaic system with three-level boosting MPPT control", IEEE Transaction Power Electronic ,vol. 23, PP. 2319–2327, Sep. 2008.
[11] M. Samadi, S.M. Rakhtala, "Design output control TLB converter for DC drive applications with photovoltaic power supply" Journal of Solar Energy Research, pp.105-110, 2017.
[12] RakhtAla SM, Yasoubi M, HosseinNia H, "Design of second order sliding mode and sliding mode algorithms: a practical insight to DC-DC buck converter" IEEE/CAA Journal of Automatica Sinica. 2017;4(3):483-97.
[13] M. H. Todorovic, L. Palma, and P. N. Enjeti, "Design of a wide input range DC–DC converter with a robust power control scheme suitable for fuel cell power conversion", IEEE Transaction Industrial Electronic, vol. 55, no. 3, PP. 1247–1255, Mar. 2008.
[14] A. Shahin, M. Hinaje, J. P. Martin, S. Pierfederici, S. Rael, and B. Davat,"High voltage ratio DC–DC converter for fuel-cell applications", IEEE Transaction Industrial Electronic, vol. 57, PP. 3944–3955, Dec. 2010.
[15] V.Yaramasu and B.Wu, "Three-Level boost converter based medium voltage megawatt PMSG wind energy conversion systems", in 2011 IEEE Energy Conversion Congress and Exposition, Phoenix, AZ, 2011, PP. 561-567.
[16] Xinbo Ruan, Bin Li, Qianhong Chen, Siew-Chong Tan and Chi K. Tse, "Fundamental Considerations of Three-Level DC–DC Converters: Topologies, Analyses, and Control", IEEE Transaction on circuits and systems, vol. 55, no. 11, Dec. 2008.
[17] L. S. Yang, T. J. Liang, H. C. Lee and J. F. Chen, "Novel High Step-Up DC–DC Converter With Coupled-Inductor and Voltage-Doubler Circuits", IEEE Transaction on Industrial Electronics, vol. 58, no. 9, PP.4196-4206, Sep. 2011.
[18] B. R. Lin and H. H. Lu, "A novel PWM scheme for single-phase three level power-factor-correction circuit", IEEE Transaction Industrial Electronic, vol. 47,no. 2, PP. 245–252, Apr. 2000.
[19] Remya Krishna, Deepak E. Soman, Sasi K. Kottayil, Mats Leijon, "Pulse delay control for capacitor voltage balancing in a three-level boost neutral point clamped inverter", IET Power Electronics., vol. 8, PP. 268 - 277, June 2015.
[20] A. Zorig, M. Belkheir, S. Barkat, "Control of Three-Level T-Type Inverter Based Grid Connected PV System",13th International Multi-Conference on Systems, Signals & Devices (SSD), May 2016.
[21] Venkata Yaramasu, Bin Wu, "Predictive Control of Three-Level Boost Converter and NPC Inverter for High Power PMSG-Based Medium Voltage Wind Energy Conversion Systems", IEEE Transactions on Power Electronics, vol.29 , PP. 5308 – 5322, Oct 2014.
[22] R. Ghosh and G. Narayanan,"A Simple Analog Controller for Single Phase Half-Bridge Rectifier", IEEE Transactions on Power Electronics, vol. 22, no. 1, PP. 186–198, Jan. 2007.

[23] B. R. Lin, T. L. Huang, and C. H. Huang, “Bi-directional single-phase half-bridge rectifier for power quality compensation”, IEE Proceedings - Electric Power Applications, vol. 150, no. 4, pp. 397-406, 8 July 2003.
[24] Z. Shu, N. Ding, J. Chen, H. Zhu, and X. He, “Multilevel SVPWM with DC-link capacitor voltage balancing control for diode-clamped multilevel converter based STATCOM”, IEEE Transaction Industrial Electronic, vol. 60, no. 5, PP. 1884–1896, May 2013.
[25] C. Gao, X. Jiang, Y. Li, Z. Chen, and J. Liu, “A DC-link voltage self-balancing method for a diode-clamped modular multilevel converter with minimum number of voltage sensors”, IEEE Transaction Industrial Electronic, vol. 28, no. 5, PP. 2125–2139, May 2013.
[26] Hung-Chi Chen and Wen-Jan Lin, “MPPT and Voltage Balancing Control With Sensing Only Inductor Current for Photovoltaic-Fed, Three-Level, Boost-Type Converters”, IEEE Transaction Industrial Electronic, vol. 29, no. 1, PP. 29-35, January 2014.
[27] V. Salas, E. Oli´s, A. Barrado and A. La´zaro, “Review of the maximum power point tracking algorithms for stand-alone photovoltaic systems”, Solar Energy Materials and Solar Cells, vol.90, no.11, PP.1555-1578, July 2006.
[28] Josean Ramos-Hernanz, Jose Manuel Lopez-Guede, Oscar Barambones, Ekaitz Zulueta, Unai Fernandez-Gamiz, "Novel control algorithm for MPPT with Boost converters in photovoltaic systems", International Journal of Hydrogen**,** PP. 1-25, 17 March 2017.
[29] Yeong-Chau Kuo, Tsorng-Juu Liang, and Jiann-Fuh Chen, “Novel Maximum-Power-Point-Tracking Controller for Photovoltaic Energy Conversion System”, IEEE Transaction Industrial Electronic, vol. 48, no. 3, PP. 594-601, June 2001.
[30] Yinqing Zoua , Youling Yua, Yu Zhangb and Jicheng Luc, “MPPT Control for PV Generation System Based on an Improved Inccond Algorithm” Procedia Engineering, vol. 29, 2012, PP.105-109, 2012.
[31] Tajuddin MF, Arif MS, Ayob SM, Salam Z, “Perturbative methods for maximum power point tracking (MPPT) of photovoltaic (PV) systems: a review” International Journal of Energy Research. 2015 Jul;39(9):1153-78.
[32] Mohammed Ali Elgendy, David John Atkinson, Bashar Zahawi, “Experimental investigation of the incremental conductance maximum power point tracking algorithm at high perturbation rates”, IET Renewable Power Generation, vol. 10, no. 2, PP. 133-139, 2016.
[33] Chih-Chiang Hua, Yi-Hsiung Fang, Wei-Tze Chen,“Hybrid maximum power point tracking method with variable step size for photovoltaic systems”, IET Renewable Power Generation, vol. 10, no. 2, PP. 127-132, 2016.
[34] Sefa I, Altin N, Ozdemir S, Kaplan O, “Fuzzy PI controlled inverter for grid interactive renewable energy systems”, IET Renewable Power Generation vol. 9 no.7, PP.729-738, 2015.
[35] M. Samadi, S.M. Rakhtala,”Reducing cost and size in photovoltaic systems using Three-level boost converter based on fuzzy logic controller” Iran J Sci Technol Trans Electr Eng, 2018 .
[36] G. Balasubramanian, S. Singaravelu, “Fuzzy logic controller for the maximum power point tracking in photovoltaic system,” International Journal of Computer Applications (0975 – 8887) Volume 41– No.12 , March 2012.
[37] Qiqi Zhao, Yu Fang, Mingming Ma, Jun Wang, Yong Xie, “Study on a Fuzzy Controller for the Balance of Capacitor Voltages of Three-Level Boost DC-DC Converter”, Conference Paper published in International Power Electronics and Application Conference and Exposition, Shanghai, PP. 993-996, 2014.
[38] Lais A Vitoi, Remya Krishna, Deepak E Soman, Mats Leijon, Sasi K Kottayil, "Control and Implementation of Three Level Boost Converter for Load Voltage Regulation", Industrial Electronics Society, IECON 2013 - 39th Annual Conference of the IEEE, pp. 561-565, Jan 2014.
[39] Abdellatif Nouri, Issam Salhi, Elmostafa Elwarraki, Said El Beid, Najib Essounbouli, "DSP-based implementation of a self-tuning fuzzy controller forthree-level boost converter", Electric Power Systems Research, vol.146, pp. 286-297, May 2017.

Author mohamadreza samadi and seyed mehdi rakhtala and morteza ahmadian alashti both act as consultants for Company Noshirvani University of Technology mentioned in the article.
Authors have no conflict of interest relevant to this article.